CAMBRIDGE
UNIVERSITY PRESS

Article

Libbyite, $(NH_4)_2(Na_2\square)[(UO_2)_2(SO_4)_3(H_2O)]_2·7H_2O$, a new mineral with uranyl–sulfate sheets from the Blue Lizard mine, San Juan County, Utah, USA

Anthony R. Kampf[1]* , Travis A. Olds[2], Jakub Plášil[3] , Barbara P. Nash[4] and Joe Marty[1]

[1]Mineral Sciences Department, Natural History Museum of Los Angeles County, 900 Exposition Boulevard, Los Angeles, CA 90007, USA; [2]Section of Minerals and Earth Sciences, Carnegie Museum of Natural History, 4400 Forbes Avenue, Pittsburgh, Pennsylvania 15213, USA; [3]Institute of Physics of the CAS, Na Slovance 1999/2, 18200 Prague 8, Czech Republic and [4]Department of Geology and Geophysics, University of Utah, Salt Lake City, UT 84112, USA

Abstract

The new mineral libbyite (IMA2022-091), $(NH_4)_2(Na_2\square)[(UO_2)_2(SO_4)_3(H_2O)]_2·7H_2O$, was found in the Blue Lizard mine, San Juan County, Utah, USA, where it occurs as tightly intergrown aggregates of light green–yellow equant crystals in a secondary assemblage with bobcookite, coquimbite, halotrichite, metavoltine, rhomboclase, römerite, tamarugite, voltaite and zincorietveldite. The streak is very pale green yellow and the fluorescence is strong green under 405 nm ultraviolet light. Crystals are transparent with vitreous lustre. The tenacity is brittle, the Mohs hardness is ∼2½, the fracture is curved. The mineral is soluble in H_2O and has a calculated density of 3.465 $g·cm^{-3}$. The mineral is optically uniaxial (–) with $\omega = 1.581(2)$ and $\varepsilon = 1.540(2)$. Electron microprobe analyses provided $(NH_4)_{1.92}K_{0.08}Na_{2.00}U_{4.00}S_{6.00}O_{41}H_{18.00}$. Libbyite is tetragonal, $P4_12_12$, $a = 10.7037(11)$, $c = 31.824(2)$ Å, $V = 3646.0(8)$ $Å^3$ and $Z = 4$. The structural unit is a uranyl–sulfate sheet that has the same topology as the sheets in several synthetic uranyl selenates.

Introduction

Of the 60 known uranyl–sulfate minerals, nearly half were first discovered during the last 10 years in the mines of Red Canyon in southeast Utah, USA. The Blue Lizard mine, in particular, has been a prolific source, and is now the type locality for 22 uranyl–sulfate minerals (see Plášil *et al.*, 2023; Kampf *et al.*, 2023a), with more awaiting characterisation. The new mineral libbyite, $(NH_4)_2(Na_2\square)[(UO_2)_2(SO_4)_3(H_2O)]_2·7H_2O$, described herein, is the latest to be described from the Blue Lizard mine. Like several of the other new uranyl sulfates from here, libbyite contains a uranyl–sulfate structural unit that has not previously been found in Nature.

Libbyite is named in honour of American nuclear chemist Willard F. Libby (1908–1980) for his work on nuclear and radiochemistry. Dr. Libby's long and illustrious career, following a Ph.D. in chemistry from the University of California at Berkeley in 1933, included chemistry professorships at UC Berkeley, the University of Chicago (Institute for Nuclear Studies) and the University of California at Los Angeles (UCLA), where he was Director of the Institute of Geophysics and Planetary Physics (IGPP). During his tenure at the University of Chicago, Dr. Libby developed the method of radiocarbon dating (published in 1952) for which he was awarded the Nobel Prize in Chemistry for 1960.

The new mineral and name (symbol Ly) were approved by the Commission on New Minerals, Nomenclature and Classification of the International Mineralogical Association (IMA2022-091, Kampf *et al.*, 2023b). The description is based on four cotype specimens, all micromounts, deposited in the collections of the Natural History Museum of Los Angeles County, 900 Exposition Boulevard, Los Angeles, CA 90007, USA, catalogue numbers 76267, 76268, 76269 and 76270. Specimen 76267 is also a cotype for zincorietveldite (Kampf *et al.*, 2023a).

Occurrence

Libbyite was found by two of the authors (ARK and JM) in efflorescent crusts on mine walls underground in the Blue Lizard mine (37°33'26"N 110°17'44"W), Red Canyon, White Canyon District, San Juan County, Utah, USA. The mine is ∼72 km west of the town of Blanding, Utah, and ∼22 km southeast of Good Hope Bay on Lake Powell. Detailed historical and geological information on the Blue Lizard mine is described elsewhere (e.g. Kampf *et al.*, 2015), and is derived primarily from a report by Chenoweth (1993). Abundant secondary uranium mineralisation in Red Canyon is associated with post-mining oxidation of asphaltite-rich sandstone beds laced with uraninite and sulfides in the damp underground environment. Libbyite is a rare mineral found in association with bobcookite, coquimbite, halotrichite, metavoltine, rhomboclase, römerite, tamarugite, voltaite, zincorietveldite and other potentially new minerals on matrix comprised

*Corresponding author: Anthony R. Kampf; Email: akampf@nhm.org

mostly of subhedral to euhedral, equant quartz crystals that are recrystallised counterparts of the original grains of the sandstone.

Morphology, physical properties and optical properties

Libbyite occurs as tightly intergrown aggregates of equant, somewhat rounded, light green–yellow crystals (Fig. 1). No crystal forms could be measured, but {001}, {011} and {111} appear likely. Merohedral twinning is likely because of the noncentrosymmetric space group, but was not observed. The streak is very pale green yellow. The mineral fluoresces strong green under 405 nm ultraviolet illumination. Crystals are transparent with vitreous lustre. The tenacity is brittle and the fracture is curved. The Mohs hardness is ~2½ based on scratch tests. Cleavage is excellent on {001}. The density could not be measured because the mineral is soluble in Clerici solution and there is insufficient material available for physical measurement. The calculated density based upon the empirical formula is 3.465 g·cm^{-3}. The mineral is easily soluble in room-temperature H_2O. Libbyite is optically uniaxial (–) with $\omega = 1.581(2)$ and $\varepsilon = 1.540(2)$ measured in white light. The pleochroism is O = yellow, E = pale yellow; $O > E$. The Gladstone–Dale compatibility (Mandarino, 2007) $1 - (K_p/K_c)$ is 0.001 (superior) based on the empirical formula using $k(UO_3) = 0.118$, as provided by Mandarino (1976).

Raman spectroscopy

Raman spectroscopy was conducted on a Horiba XploRA PLUS using a 100× (0.9 NA) objective. Libbyite was very sensitive to the 532 nm diode laser and exhibited strong fluorescence. Consequently, the spectrum from 2000 to 60 cm^{-1} was recorded with a 785 nm laser (100 µm slit and 1800 gr/mm diffraction grating). The spectrum was featureless between 2000 and 1300 cm^{-1} so only the spectrum from 1300 and 100 cm^{-1} is shown in Fig. 2. The approximate wavenumbers and tentative band assignments are labelled in the expanded portion of Fig. 2. The band assignments are based primarily upon those for uranyl–sulfate minerals provided by Čejka (1999) and Plášil *et al.* (2010).

The presence of three symmetrically distinct SO_4 tetrahedra in the structure of libbyite leads to the multiple split bands for the SO_4 modes. According to the empirical relationship of Bartlett
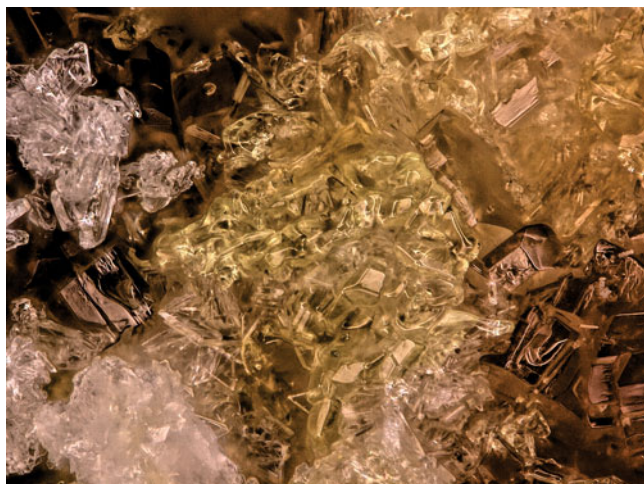

Figure 1. Libbyite with römerite (mauve) and tamarugite (colourless) on specimen #76267. The field of view is 0.68 mm across.

and Cooney (1989), the very strong ν_1 $(UO_2)^{2+}$ symmetric stretching vibration at 864 cm^{-1} corresponds to an approximate U–O$_{Ur}$ bond length of 1.75 Å, in good agreement with the average U1–O$_{Ur}$ bond length from the X-ray data: 1.765 Å.

Chemical composition

Electron probe microanalyses (EPMA) were performed at the University of Utah on a Cameca SX-50 electron microprobe with four wavelength dispersive spectrometers and using *Probe for EPMA* software. Analytical conditions were 15 kV accelerating voltage, 10 nA beam current and 10 µm beam diameter and 3 points were analysed. Raw X-ray intensities were corrected for matrix effects with a $\phi\rho(z)$ algorithm (Pouchou and Pichoir, 1991). No other elements were detected. There was major beam damage and, despite efforts to apply time-dependent corrections, it was obvious that they could not account for major rapid losses of N and Na. Consequently, we calculated $(NH_4)_2O$ and Na_2O based on the ideal formula (see below). The significant H_2O loss under vacuum and during analyses resulted in higher concentrations for the remaining constituents than are to be expected for the fully hydrated phase; therefore, the other analysed constituents have been normalised to provide a total of 100% when combined with the calculated H_2O content. Analytical data are given in Table 1.

The empirical formula (calculated on the basis of 41 O atoms per formula unit) is $(NH_4)_{1.92}K_{0.08}Na_{2.00}U_{4.00}S_{6.00}O_{41}H_{18.00}$. The simplified formula is $(NH_4,K)_2(Na,\square)_3[(UO_2)_2(SO_4)_3(H_2O)]_2 \cdot 7H_2O$ and the ideal formula is $(NH_4)_2(Na_2\square)[(UO_2)_2(SO_4)_3(H_2O)]_2 \cdot 7H_2O$, which requires $(NH_4)_2O$ 2.74, Na_2O 3.26, UO_3 60.20, SO_3 25.27, H_2O 8.53, total 100 wt.%.

X-ray crystallography

Powder X-ray diffraction (PXRD) data were recorded using a Rigaku R-Axis Rapid II curved imaging plate microdiffractometer with monochromatised MoKα radiation. A Gandolfi-like motion on the φ and ω axes was used to randomise the sample. Observed d values and intensities were derived by profile fitting using *JADE Pro* software (Materials Data, Inc.). The powder data are presented in Supplementary Table S1. The unit-cell parameters refined from the powder data using *JADE Pro* with whole pattern fitting are $a = 10.7032(18)$, $c = 31.864(6)$ Å and $V = 3650.3(1)$ Å^3.

The single-crystal structure data were collected at room temperature using the same diffractometer and radiation noted above. The best crystal found exhibited relatively high mosaicity. The mosaicity coupled with the close spacing of reflections along **c** caused problems in integration, which, in turn, forced us to drop some frames. This is the cause of the rather low completeness value of 92.7%. The structure data for libbyite were processed using the Rigaku *CrystalClear* software package, including the application of an empirical multi-scan absorption correction using *ABSCOR* (Higashi, 2001). The structure was solved using *SHELXT* (Sheldrick, 2015a). Refinement proceeded by full-matrix least-squares on F^2 using *SHELXL-2016* (Sheldrick, 2015b). The large b parameter in the final weighting function reflects the relatively low quality of the data. Data collection and refinement details are given in Table 2, atom coordinates and displacement parameters in Table 3, selected bond distances in Table 4 and a bond-valence analysis in Table 5. The crystallographic information file has been deposited with the Principal Editor of
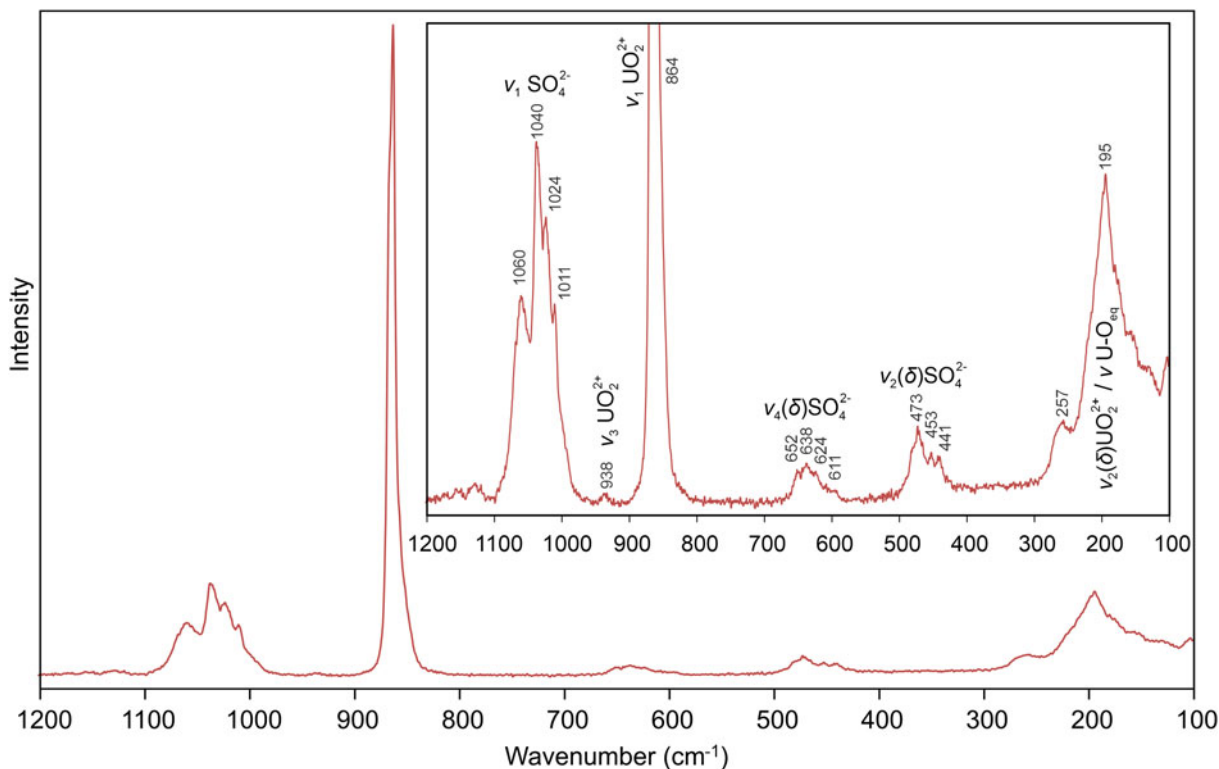
Figure 2. The Raman spectrum of libbyite recorded with a 785 nm laser.

Mineralogical Magazine and is available as Supplementary material (see below).

Description of the structure

Two U sites (U1 and U2) in the structure of libbyite are each surrounded by seven O atoms forming squat UO_7 pentagonal bipyramids. This is a typical coordination for U^{6+} in which the two short apical bonds of the bipyramid constitute the uranyl group (see Burns, 2005). The two apical O atoms of the bipyramids (O_{Ur}) form short bonds with the U, and this unit comprises the UO_2^{2+} uranyl group. Five equatorial O atoms (O_{eq}) complete the U coordinations.

There are three S sites (S1, S2 and S3) each centring an SO_4 tetrahedron. The SO_4 tetrahedra share corners with the equatorial O atoms of the UO_7 bipyramids to form a uranyl–sulfate sheet with the composition $[(UO_2)_2(SO_4)_3(H_2O)]^{2-}$ (Fig. 3). Within this sheet, the U1 bipyramid shares four of its O_{eq} corners with SO_4 groups and the U2 bipyramid shares all five of its O_{eq} corners

with SO_4 groups. The uranyl–sulfate sheet in the structure of libbyite is unique in the mineral kingdom, however it has the same topology as the sheet in the synthetic phase $K(H_5O_2)$

Table 1. Analytical data (in wt.%) for libbyite.

Constituent	Mean	Range	S.D.	Standard	Normalised
$(NH_4)_2O$	1.27	1.11–1.43	0.10	syn. Cr_2N	2.63*
K_2O	0.22	0.21–0.23	0.01	sanidine	0.21
Na_2O	2.50	2.00–2.75	0.44	albite	3.26*
UO_3	62.83	62.37–63.13	0.41	syn. UO_2	60.12
SO_3	26.39	25.93–26.59	0.40	celestine	25.25
H_2O					8.52*
Total					99.99

* Based on N + K = 1, Na = 2 and O = 41 apfu.
S.D. = standard deviation.

Table 2. Data collection and structure-refinement details for libbyite.

Crystal data	
Structural formula	$[(NH_4)_{1.75}K_{0.25}](Na_{2.81}\square_{0.19})$ $[(UO_2)_2(SO_4)_3(H_2O)]_2\cdot 7H_2O$ (including unlocated H atoms)
Space group	$P4_12_12$ (#92)
Unit cell dimensions (Å)	$a = 10.7037(11)$, $c = 31.824(2)$
V (Å^3)	3646.0(8)
Z	4
Density (for above formula) (g·cm^{-3})	3.468
Absorption coefficient (mm^{-1})	18.249
$F(000)$	3377.4
Data collection	
Diffractometer	Rigaku R-Axis Rapid II
X-ray radiation/power	Mo$K\alpha$ ($\lambda = 0.71075$ Å)/50 kV, 40 mA
Temperature (K)	293(2)
Crystal size (μm)	160 × 65 × 20
θ range	3.19 to 25.02°
Index ranges	$-11 \le h \le 11$, $-10 \le k \le 12$, $-37 \le l \le 37$
Reflections collected/unique	13889/2829; $R_{int} = 0.096$
Reflections with $I > 2\sigma I$	2421
Completeness to $\theta = 25.02°$	92.7%
Refinement	
Refinement method	Full-matrix least-squares on F^2
Parameters/restraints	236/0
GoF	1.120
Final R indices [$I > 2\sigma I$]	$R_1 = 0.0576$, $wR_2 = 0.1480$
R indices (all data)	$R_1 = 0.0718$, $wR_2 = 0.1676$
Absolute structure parameter	0.017(13)
Largest diff. peak/hole ($e^-\cdot A^{-3}$)	+2.26/−3.83

$R_{int} = \Sigma|F_o^2-F_o^2(\text{mean})|/\Sigma[F_o^2]$. GoF = $S = \{\Sigma[w(F_o^2-F_c^2)^2]/(n-p)\}^{1/2}$. $R_1 = \Sigma||F_o|-|F_c||/\Sigma|F_o|$. $wR_2 = \{\Sigma[w(F_o^2-F_c^2)^2]/\Sigma[w(F_o^2)^2]\}^{1/2}$; $w = 1/[\sigma^2(F_o^2)+(aP)^2+bP]$ where a is 0.0739, b is 169.7151 and P is $[2F_c^2+\text{Max}(F_o^2,0)]/3$.

Table 3. Atom coordinates and displacement parameters (Å^2) for libbyite.

	x/a	y/b	z/c	U_{eq}	U^{11}	U^{22}	U^{33}	U^{23}	U^{13}	U^{12}
N*	0.636(4)	0.971(3)	0.7294(8)	0.071(16)	0.12(3)	0.05(2)	0.044(18)	0.000(13)	−0.023(18)	0.01(2)
Na1	0.3845(19)	0.6155(19)	0.75	0.058(7)	0.056(11)	0.056(11)	0.062(15)	−0.003(8)	−0.003(8)	−0.021(14)
Na2*	0.1069(15)	0.780(2)	0.5237(5)	0.046(7)	0.021(10)	0.079(16)	0.039(10)	0.009(8)	−0.008(6)	−0.013(9)
U1	0.63108(12)	0.25270(12)	0.62550(4)	0.0268(4)	0.0295(7)	0.0284(7)	0.0225(6)	−0.0011(5)	0.0015(5)	0.0010(6)
U2	0.35609(13)	0.85571(13)	0.61905(3)	0.0274(4)	0.0295(7)	0.0290(8)	0.0237(6)	−0.0003(5)	0.0001(5)	0.0002(6)
S1	0.4341(9)	0.5242(9)	0.6358(3)	0.031(2)	0.036(6)	0.030(5)	0.027(4)	−0.001(3)	0.001(3)	−0.009(5)
S2	0.6523(10)	0.9482(9)	0.5704(2)	0.031(2)	0.042(6)	0.031(5)	0.019(4)	0.002(3)	0.001(4)	0.007(5)
S3	0.3651(9)	0.1681(8)	0.5643(2)	0.0270(19)	0.030(5)	0.028(5)	0.023(4)	0.001(3)	−0.001(3)	0.008(4)
O1	0.421(2)	0.505(2)	0.6797(7)	0.032(6)	0.025(14)	0.034(16)	0.038(14)	0.000(11)	−0.003(10)	0.001(13)
O2	0.457(2)	0.659(2)	0.6268(6)	0.024(5)						
O3	0.323(2)	0.480(3)	0.6119(7)	0.036(6)	0.040(16)	0.046(17)	0.022(12)	0.002(10)	−0.009(10)	0.000(13)
O4	0.551(2)	0.462(2)	0.6194(6)	0.022(5)						
O5	0.638(3)	0.006(3)	0.5292(7)	0.048(8)	0.07(2)	0.045(17)	0.029(13)	0.009(11)	−0.006(14)	−0.008(17)
O6	0.652(3)	0.037(3)	0.6053(8)	0.040(7)	0.029(15)	0.043(17)	0.049(15)	−0.026(13)	−0.002(12)	0.003(15)
O7	0.771(2)	0.880(2)	0.5717(7)	0.030(6)	0.007(11)	0.040(16)	0.042(13)	0.008(11)	0.003(9)	0.011(12)
O8	0.549(2)	0.858(2)	0.5778(7)	0.027(5)	0.034(14)	0.015(12)	0.034(12)	0.000(10)	0.021(10)	−0.005(12)
O9	0.347(3)	0.150(3)	0.5205(8)	0.057(9)	0.047(18)	0.09(3)	0.036(13)	−0.010(15)	0.001(12)	−0.043(19)
O10	0.375(3)	0.051(3)	0.5854(9)	0.056(10)	0.06(2)	0.042(18)	0.069(19)	0.042(15)	0.027(15)	0.039(17)
O11	0.260(3)	0.238(3)	0.5816(8)	0.054(8)	0.06(2)	0.040(18)	0.063(16)	0.018(14)	0.039(16)	0.013(18)
O12	0.483(2)	0.245(2)	0.5715(7)	0.037(6)	0.060(19)	0.014(13)	0.036(13)	0.004(11)	−0.015(11)	−0.012(14)
O13	0.521(2)	0.215(2)	0.6647(6)	0.022(5)						
O14	0.746(3)	0.297(3)	0.5886(7)	0.045(8)	0.038(16)	0.07(2)	0.028(12)	−0.003(11)	0.014(12)	0.002(17)
O15	0.437(2)	0.917(2)	0.6622(6)	0.030(5)						
O16	0.273(3)	0.794(2)	0.5753(7)	0.036(7)	0.032(15)	0.041(17)	0.036(13)	−0.012(11)	−0.005(11)	0.000(13)
OW1	0.797(2)	0.141(3)	0.6653(7)	0.032(6)	0.019(13)	0.040(16)	0.038(13)	0.003(12)	0.001(9)	0.013(13)
OW2	0.580(3)	0.710(2)	0.7294(8)	0.044(7)	0.08(2)	0.012(13)	0.040(14)	0.002(10)	0.011(14)	0.005(14)
OW3	0.913(3)	0.913(3)	0.500000	0.046(10)	0.046(17)	0.046(17)	0.05(2)	−0.006(11)	0.006(11)	0.02(2)
OW4	0.238(3)	0.568(3)	0.5241(7)	0.049(8)	0.08(2)	0.039(17)	0.029(13)	−0.006(11)	−0.003(14)	−0.029(17)
OW5	0.478(3)	0.635(5)	0.5094(13)	0.096(15)	0.014(16)	0.14(4)	0.13(3)	−0.03(3)	0.018(18)	0.01(2)

* Refined occupancies: N = N$_{0.88(6)}$/K$_{0.12(6)}$; Na2 = 0.90(6)

$[(UO_2)_2(SeO_4)_3(H_2O)]$ (Gurzhiy *et al.*, 2012) and as those in seven other synthetic uranyl selenates listed by Krivovichev (2009) with graph cc2–2:3–4 and ring symbol $4^3 6^1$. The charge-deficiency-per-anion (*CDA*), which is one of the useful measures to quantify the bond-valence characteristics of the structural units of minerals, is 0.14 valence units for libbyite. It is noteworthy that the value found for such an 'exotic' sheet is not far from the *CDA* values observed for other sheet uranyl sulfates, for example, for some of the zippeite group of minerals (see Plášil *et al.*, 2023).

The region between the uranyl–sulfate sheets (Fig. 4) contains one NH$_4$ site (N), two Na sites (Na1 and Na2) and four H$_2$O sites (OW2, OW3, OW4 and OW5). The NH$_4$ site is seven coordinated (for N–O < 3.3 Å). The Na1 site is six coordinated and the Na2 site is seven coordinated. The sheets are linked to each other in the [001] direction via NH$_4$–O, Na–O and hydrogen bonds.

The structural formula, $[(NH_4)_{1.75}K_{0.25}](Na_{2.81}\square_{0.19})[(UO_2)_2(SO_4)_3(H_2O)]_2 \cdot 7H_2O$, based on our refinement has an excess positive charge of 0.81. In the final stages of refinement, we allowed interlayer cation occupancies to refine freely for an

Table 4. Selected bond distances (Å) for libbyite.

						Hydrogen bonds	
NH$_4$–OW5	2.63(6)	U1–O13	1.76(2)	S1–O1	1.42(3)		
NH$_4$–O5	2.84(5)	U1–O14	1.77(3)	S1–O2	1.49(2)	OW1···O4	2.75(3)
NH$_4$–OW2	2.86(4)	U1–O12	2.34(2)	S1–O3	1.49(3)	OW1···O8	2.85(4)
NH$_4$–O15	3.08(4)	U1–O6	2.40(2)	S1–O4	1.51(2)	OW2···O9	3.15(4)
NH$_4$–O14	3.12(4)	U1–O4	2.40(2)	<S1–O>	1.48	OW2···O14	3.00(3)
NH$_4$–OW1	3.23(4)	U1–O7	2.40(3)			OW3···O5 (×2)	3.25(4)
NH$_4$–O8	3.24(4)	U1–OW1	2.49(2)	S2–O5	1.46(2)	OW4···O5	3.10(4)
<NH$_4$–O>	3.00	<U1–O$_{Ur}$>	1.77	S2–O6	1.46(2)	OW4···O9	2.91(4)
		<U1–O$_{eq}$>	2.41	S2–O7	1.47(2)	OW5···OW4	2.70(5)
Na1–OW2 (×2)	2.41(3)			S2–O8	1.49(2)	OW5···OW5	2.45(8)
Na1–O1 (×2)	2.56(3)	U2–O15	1.75(2)	<S2–O>	1.47		
Na1–O9 (×2)	2.59(4)	U2–O16	1.78(2)				
<Na1–O>	2.52	U2–O10	2.36(3)	S3–O9	1.42(3)		
		U2–O11	2.37(3)	S3–O10	1.43(3)		
Na2–OW2	2.34(3)	U2–O2	2.38(2)	S3–O11	1.46(3)		
Na2–O16	2.42(3)	U2–O3	2.41(3)	S3–O12	1.52(3)		
Na2–O13	2.49(3)	U2–O8	2.45(2)	<S3–O>	1.46		
Na2–O5	2.51(3)	<U2–O$_{Ur}$>	1.77				
Na2–OW3	2.63(2)	<U2–O$_{eq}$>	2.39				
Na2–OW4	2.67(4)						
Na2–O1	2.85(3)						
<Na2–O>	2.56						

Table 5. Bond valence analysis for libbyite. Values are expressed in valence units.*

	NH₄	Na1	Na2	U1	U2	S	S2	S3	Hydrogen bonds	Σ
O1		0.13×2↓	0.06			1.71				1.90
O2					0.49	1.43				1.93
O3					0.46	1.43				1.90
O4				0.47		1.36			0.20	2.04
O5	0.19		0.14				1.55		0.10, 0.11	1.90
O6					0.47		1.55			2.02
O7				0.47			1.51			1.98
O8	0.06				0.43		1.43		0.17	2.03
O9		0.12×2↓						1.71	0.11, 0.15	1.97
O10					0.51			1.67		2.18
O11					0.50			1.55		2.05
O12				0.54				1.33		1.87
O13			0.15	1.83						1.98
O14	0.09				1.79				0.13	1.92
O15	0.10				1.87					1.87
O16			0.18		1.75					1.93
OW1	0.07			0.39					−0.20, −0.17	0.02
OW2	0.18	0.18×2↓	0.22						−0.11, 0.13	0.34
OW3			0.11, 0.11						−0.10, −0.10	0.02
OW4			0.10						−0.11, −0.15, 0.23	0.06
OW5	0.33		0.06						−0.23, −0.43, 0.43	0.10
Σ	1.01	0.86	0.93	5.96	6.01	5.93	6.04	6.26		

*NH₄⁺–O bond valence parameters are from García-Rodríguez *et al.* (2000); U⁺⁶–O and S⁺⁶–O bond-valence parameters are from Gagné and Hawthorne (2015). Hydrogen-bond strengths based on O–O bond lengths are from Ferraris and Ivaldi (1988). Negative values indicate donated hydrogen-bond contributions.

indication of their preferred site occupancies. The Na1 site refined to full occupancy and the Na2 site to 0.90 occupancy; however, both Na sites, as well as the NH₄ site, exhibited large anisotropic displacement parameters. This suggests that the total of the refined Na and NH₄ site occupancies is larger than reality. To test this, a refinement was done with the site occupancies adjusted to Na1: 0.62, Na2: 0.69, N: $N_{0.96}K_{0.04}$ corresponding to the structural formula $[(NH_4)_{1.92}K_{0.08}](Na_{2.00}\square_{1.00})[(UO_2)_2(SO_4)_3(H_2O)]_2 \cdot 7H_2O$, which is the same as the EPMA empirical formula. The refinement was well behaved, converging to $R_1 = 0.0590$, with reasonable U_{eq} values of 0.022, 0.027 and 0.055 for the Na1, Na2 and N sites, respectively.

Electron probe microanalysis of libbyite was very challenging because the mineral is very sensitive to the electron beam.

Preliminary energy dispersive spectroscopy (EDS) indicated sufficient N to account for full occupancy of the NH₄ site in the structure and the structure refinement indicated full occupancy of the site together with greater K than indicated by the EPMA. The preliminary EDS also indicated ∼2.5 Na atoms per formula unit. Considering the results of the structure refinement noted in the previous paragraph, we believe that the most realistic ideal formula for libbyite is $(NH_4)_2(Na_2\square)[(UO_2)_2(SO_4)_3(H_2O)]_2 \cdot 7H_2O$.

New structure types such as those found in libbyite provide important metrics when surveying for potential relationships between the observed crystal chemistry and the, usually unmeasured, conditions of formation. The diverse and densely co-mingled associations of uranyl sulfates have so far made the
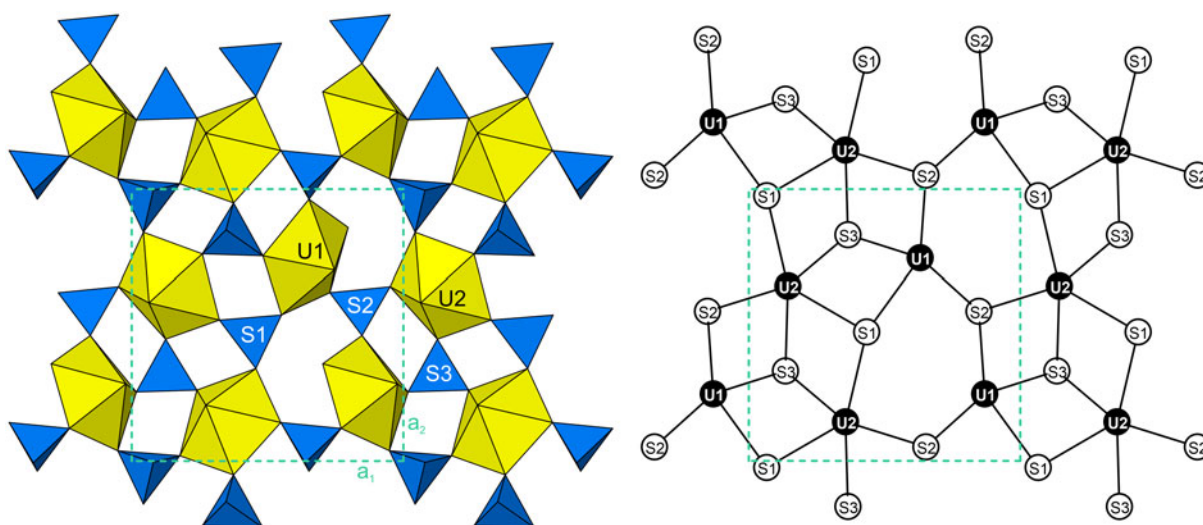

Figure 3. The $[(UO_2)_2(SO_4)_3(H_2O)]^{2-}$ sheet in libbyite viewed down [001] (left). The graph of the U and S nodes (right). The unit-cell outline is indicated by dashed green lines. Drawn using *ATOMS* (Dowty 2016).
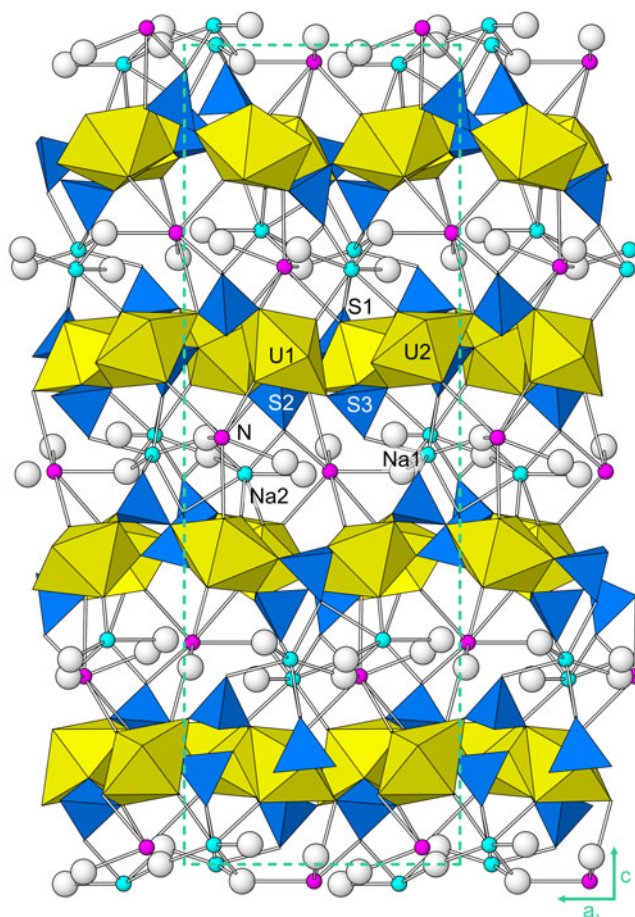
Figure 4. The crystal structure of libbyite viewed down [010]. O atoms of interlayer H$_2$O groups are white balls. The unit-cell outline is indicated by dashed green lines. Drawn using *ATOMS* (Dowty, 2016).

determination of paragenesis and the measurement of conditions of formation impossible for most species. However such an understanding is valuable when evaluating the long-term disposal of nuclear waste for certain proposed repositories, where highly soluble uranyl–sulfate minerals could form and enhance radionuclide mobility. The rarest Red Canyon uranyl sulfates occur in just one or two specimens that were confined to a very small footprint of efflorescence underground, and have afforded only a few crystals for analyses, limiting our understanding of chemical and substitutional variability. Most species have yet to be reproduced synthetically and recent efforts to do so proceed essentially by luck, with little guidance from Nature. These difficulties necessitate continued underground collecting of uranyl sulfates, together with solution data that may complement synthetic work. Sadly, recent closures of mines in Red Canyon prevent this research.

References

Bartlett J.R. and Cooney R.P. (1989) On the determination of uranium-oxygen bond lengths in dioxouranium(VI) compounds by Raman spectroscopy. *Journal of Molecular Structure*, **193**, 295–300.

Burns P.C. (2005) U^{6+} minerals and inorganic compounds: Insights into an expanded structural hierarchy of crystal structures. *The Canadian Mineralogist*, **43**, 1839–1894.

Čejka J. (1999) Infrared spectroscopy and thermal analysis of the uranyl minerals. Pp. 521–622 in: *Uranium: Mineralogy, Geochemistry, and the Environment* (P.C. Burns and R. Finch, editors). Reviews in Mineralogy, **38**. Mineralogical Society of America, Washington, DC.

Chenoweth W.L. (1993) The geology and production history of the uranium deposits in the White Canyon Mining District, San Juan County, Utah. *Utah Geological Survey Miscellaneous Publication*, 93–3.

Dowty E. (2016) *ATOMS (Version 6.5.0)*. Shape Software, Kingsport, Tennessee, USA.

Ferraris G. and Ivaldi G. (1988) Bond valence vs bond length in O···O hydrogen bonds. *Acta Crystallographica*, **B44**, 341–344.

Gagné O.C. and Hawthorne F.C (2015) Comprehensive derivation of bond valence parameters for ion pairs involving oxygen. Acta *Crystallographica*, **B71**, 562–578.

García-Rodríguez L., Rute-Pérez Á., Piñero J.R. and González-Silgo C. (2000) Bond-valence parameters for ammonium-anion interactions. *Acta Crystallographica*, **B56**, 565–569.

Gurzhiy V.V., Tyumentseva O.S., Krivovichev S.V., Tananaev I.G. and Myasoedov B.F. (2012) Synthesis and structural studies of a new potassium uranyl selenate K(H$_5$O$_2$)[(UO$_2$)$_2$(SeO$_4$)$_3$(H$_2$O)] with strongly deformed layers. *Radiochemistry*, **54**, 43–47.

Higashi T. (2001) *ABSCOR*. Rigaku Corporation, Tokyo.

Kampf A.R., Plášil J., Kasatkin A.V. and Marty J. (2015) Bobcookite, NaAl (UO$_2$)$_2$(SO$_4$)$_4$·18H$_2$O, and wetherillite, Na$_2$Mg(UO$_2$)$_2$(SO$_4$)$_4$·18H$_2$O, two new uranyl sulfate minerals from the Blue Lizard mine, San Juan County, Utah, USA. *Mineralogical Magazine*, **79**, 695–714.

Kampf A.R., Olds T.A., Plášil J. and Marty J. (2023a) Zincorietveldite, Zn (UO$_2$)(SO$_4$)$_2$(H$_2$O)$_5$, the zinc analogue of rietveldite from the Blue Lizard mine, San Juan County, Utah, USA. *Mineralogical Magazine*, **87**, https://doi.org/10.1180/mgm.2023.14

Kampf A.R., Olds T.A., Plášil J., Nash B.P. and Marty J. (2023b) Libbyite, IMA 2022-091. CNMNC Newsletter 70. *Mineralogical Magazine*, **87**, 160–168.

Krivovichev S.V. (2009) Structural crystallography of inorganic oxysalts. *IUCr Monographs on Crystallography*, **22**, 308 pp.

Mandarino J.A. (1976) The Gladstone-Dale relationship – Part 1: derivation of new constants. *The Canadian Mineralogist*, **14**, 498–502.

Mandarino J.A. (2007) The Gladstone–Dale compatibility of minerals and its use in selecting mineral species for further study. *The Canadian Mineralogist*, **45**, 1307–1324.

Plášil J., Buixaderas E., Cejka J., Sejkora J., Jehlicka J. and Novak M. (2010) Raman spectroscopic study of the uranyl sulphate mineral zippeite: low wavenumber and U-O stretching regions. *Analytical and Bioanalytical Chemistry*, **397**, 2703–2715.

Plášil J., Kampf A.R., Ma C. and Desor J. (2023) Oldsite, K$_2$Fe^{2+}[(UO$_2$) (SO$_4$)$_2$]$_2$(H$_2$O)$_8$, a new uranyl sulfate mineral from Utah, USA: its description and implications for the formation and occurrences of uranyl sulfate minerals. *Mineralogical Magazine*, **87**, 151–159, https://doi.org/10.1180/mgm.2022.106

Pouchou J.-L. and Pichoir F. (1991) Quantitative Analysis of Homogeneous or Stratified Microvolumes Applying the Model "PAP." Pp. 31–75 in: *Electron Probe Quantitation*. Springer US, Boston, USA.

Sheldrick G.M. (2015a) SHELXT – Integrated space-group and crystal-structure determination. *Acta Crystallographica*, **A71**, 3–8.

Sheldrick G.M. (2015b) Crystal structure refinement with *SHELX*. *Acta Crystallographica*, **C71**, 3–8.